Mechanics and Mechanical Engineering
Vol. 15, No. 2 (2011) 133–148

Local Dynamic Buckling of C–Shape Profile Subjected to Bending

Mariusz URBANIAK
Tomasz KUBIAK
Department of Strength of Materials and Structures
Technical University of Łódź,
Stefanowskiego 1/15, Łódź, Poland

Received (10 May 2011)
Revised (25 May 2011)
Accepted (8 June 2011)

This paper deals with local dynamic buckling of thin–walled girder segments (short beam–columns) subjected to bending. Various shapes of pulse loading (triangle, trapezoid and rectangle) with a duration corresponding to the fundamental period of vibration were taken into account. Assumed boundary conditions correspond to a simple support, this agrees with conditions that exist in the place of the diaphragm in a long spar. The problem was solved by finite element method. In order to determine the critical load pulse amplitudes Volmir, Budiansky–Hutchinson, Ari–Gur and Simonetta criteria were employed.

Keywords: Thin–walled structures, dynamic buckling, pulse loading, C–shape girders

1. Introduction

The phenomenon of stability loss has been known for over 250 years – Leonhard Euler was the first, who made an attempt to solve the buckling problem of the long rod. Destruction of such rod is determined by the critical load, above which the structure is transferred to unstable equilibrium path that leads to failure. In the recent years, considerable efforts have been put into studying the concept of stability of plates, shells and constructions (thin–walled beams, beam–columns, cylindrical or conical shell).

Pioneer works concerning this topic were carried out by Timoshenko [4] and Volmir [5]. These cases involved statically loaded thin–walled structure. Already in the 60's of twentieth century, it was proved that such structures behave differently when exposed to dynamic loads. First studies on dynamic buckling can be found in publications performed by Volmir [6] and Budiansky [7], [8].

Thin–walled structures are widely used in building structures such as thin–walled vessels or storage towers, beam–columns of houses and halls. These types of structures are also used as components for cars, boats or airplanes.

Widespread application of thin–walled elements and the strong demand for new solutions brought about development of theory and experimental researches not only on stability, post buckling behaviour and load–carrying capacity, but also on the behaviour of thin–walled structures dynamically loaded. The nature of the phenomena occurring in the case of the pulse load depends not only on the pulse duration but also on its amplitude.

The impact takes place when the pulse is characterized by very short duration and high amplitude. The dynamic load, which is studied in this paper, occurs when the pulse duration is comparable with the period of fundamental natural vibrations of the structure and the amplitude reaches medium value. Quasi–static loading corresponds to pulses with long durations.

The time depending load may be of different shape (sinusoidal, rectangular, triangular, and exponential) and have different characteristics (regular or irregular) [1]. Various pulse shapes are assumed in such a way to simulate real load [2], [3].

First publications dealing with the dynamic stability of rods are given in papers [9], [10]. Stability of thin shells, which have unstable post buckling equilibrium path, is discussed in [6], [7], [8], [11], [12], and [13]. Investigations of thin plates were presented by Volmir [6] Weller, Abramovich and Yaffe'a [14], Abramovich and Grunwald [15], Ari–Gur and Simonetta [16] or Kubiak [20]. Simitses [17] found that for plates, which have stable post buckling equilibrium path, it is not precise to consider dynamic stability loss but rather dynamic response of the load pulse is more adequate. The dynamic response is described by strengthening the amplitude of initial geometrical imperfection.

It is well known that equilibrium path for plates with initial geometrical imperfection have no bifurcation points, so the critical buckling dynamic characteristic quantity cannot be clearly defined. Therefore, it is necessary to define the criteria [18] allowing to designate critical amplitude of the pulse load. The most common criteria are as follows: Volmir criterion [6], Budiansky criterion [7], Ari–Gur criterion [16] or Petry–Fahlbush one [19]. Works related to dynamic buckling of thin–walled structures made of thin flat isotropic as well as orthotropic plates have been published in [21], [22], [23], [24].

All the works mentioned above deal with thin-walled structures subjected to axial compression or pressure load. Papers dealing with dynamic buckling of the thin–walled structures subjected to twisting and bending can also be found [21]. However, the above paper deals only with simply supported plate subjected to load corresponding to cross-section forces which was determined in the wall modelling the girder subjected to twisting and bending.

In the world of literature there exists deficiency in studies concerning thin–walled structures loaded in a complex way. Authors of this paper decided to take into account the thin–walled beams–columns with open cross–section subjected to bending moment pulse loading (compressed web, plate bended flanges).

2. Formulation of the problem

In order to understand the phenomena occurring in girders with open cross–section subjected to bending moment pulse loading numerical analysis was performed and used as a cognitive tool. The local dynamic buckling phenomenon was of major concern – this was a reason that only short segments of lengths corresponding to the formation of a single half-wave sine wave at static loads were considered.

The numerical survey was conducted to evaluate the influence of pulse shape, mode and amplitude of initial imperfections on the dynamic response of channel sections subjected to bending. With the aim of determining the critical load pulse amplitude one of the three well–known criteria of stability were used (Volmir [6], Budiansky–Hutchinson [8], Ari–Gur and Simonetta [16]). The choice of criteria for a particular case depended on obtained results. The Volmir criterion [6] assumes that the stability loss of the plates occurs when the maximum deflection is equal to a fixed value. Major assumptions consider critical values of displacement are equal to thickness or half thickness of the plate (in this paper one thickness was assumed).

The Budiansky–Hutchinson [8] criterion states that the dynamic stability loss occurs when the maximum deflection grows rapidly with the small variation of the load amplitude. One of the Ari–Gur - Simonetta [16] criterion says that the dynamic buckling occurs when a small increase in the pulse intensity causes a decrease in the peak lateral deflection. Similarly to the other works that deal with dynamic buckling the dynamic load factor DLF defined as the ratio of the pulse amplitude to the static buckling load was introduced.

The critical dynamic load factor (DLF_{cr}), at which the dynamic buckling occurs was determined using criteria mentioned above. The numerical calculations were performed for exemplary thin–walled girder with C–shape cross–section (Fig.1) with the following dimension: $b_1 = 50$ mm, $b_2 = 25$ mm, $h = 0.5$ mm, length of the column $l = 50$ mm. The material properties were assumed to be the same as for steel: $E = 2 \cdot 10^5$ MPa, $\upsilon = 0.3$. The problem was solved in the elastic range.

The scheme of the load is presented in Fig. 2. vector of the bending moment is located in the plane perpendicular to the plane of symmetry of the web.

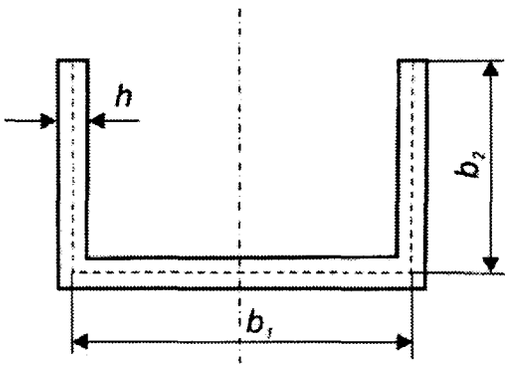

Figure 1 The loading scheme

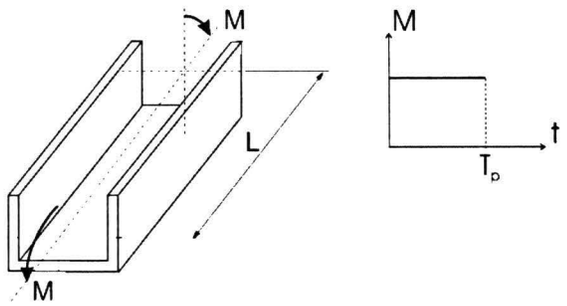

Figure 2 The loading scheme

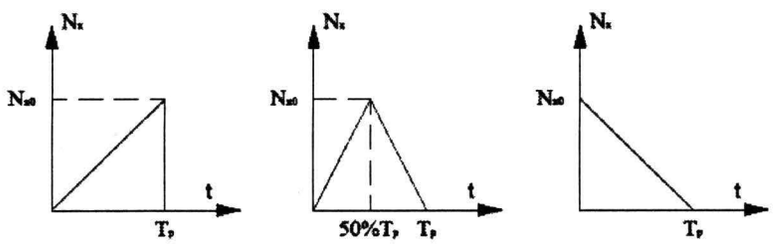

Figure 3 Triangle shapes of pulse loading: a) T1, b) T2, c) T3

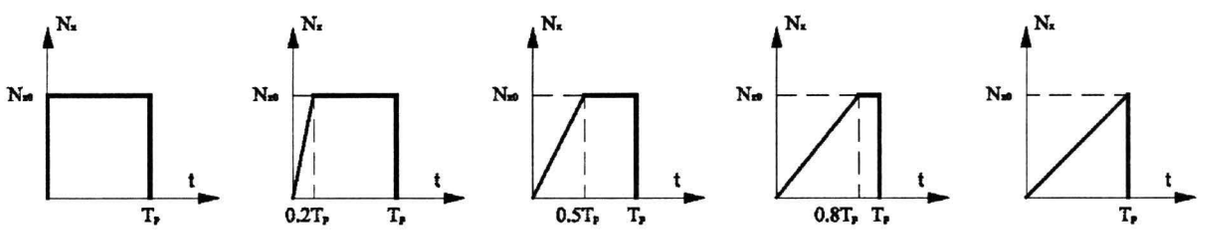

Figure 4 Transition from a rectangular to triangular T1 pulse shape

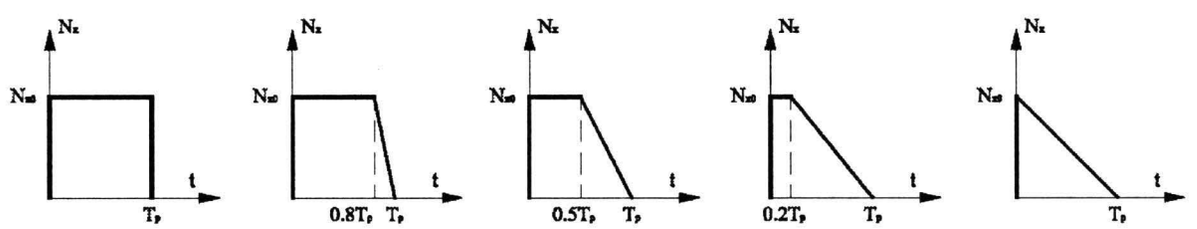

Figure 5 Transition from a rectangular to triangular T3 pulse shape

In order to investigate the influence of the shape of pulse loading on dynamic response the following pulse shapes were taken into account: rectangular (Fig. 4a), three triangular (Fig. 3 – two right triangles denotes as $T1$ and $T3$ and isosceles triangle denoted as $T2$) and three trapezoids (Fig.4b–d and Fig.5b–d) with the length of the upper base representing 20%, 50% and 80% of the length of the lower base. Pulse shapes and applied indication is given in Figs 3 to 5. It was assumed that the pulse duration is equal to the period of natural vibrations of girder under consideration. The adoption of such pulse shapes measure the effect of load increase (transition from a rectangular pulse through a trapezoidal to triangular T1 – Fig. 4) or decrease (transition from a rectangular pulse through a trapezoidal to triangular T3 – Fig. 5) on the dynamic response of girder under consideration. It should be noted that areas under pulse shape curves in Fig. 4 and Fig. 5 are different, because of their shape, duration as well as amplitude in all cases is unchangeable.

3. Numerical model

The problem was solved using finite element method, employing commercial software *ANSYS*. At the first step the eigenvalue problem was solved to find the frequencies of natural vibration with corresponding modal mode and to find critical load with corresponding buckling mode. The pulse duration T_p was set based on period of natural vibration. The critical load – in this case the critical moment M_{cr} was used to determine the dynamic load factor *DLF*. The buckling or modal mode was used to set the initial imperfection with the amplitude corresponding to the thickness of the considered girder wall. The dimensionless amplitude of initial imperfection was assumed as $\xi^* = 0; 0.01\ w_{max}/h;\ 0.1\ w_{max}/h$. The amplitude of initial imperfection set to zero ($\xi^* = 0$) means that ideal structures with flat wall were taken into consideration. The results of these calculations were used as input to the analysis of the dynamic behaviour of the structure in time, during and immediately after exposure of pulsed loads. In the analysis of the dynamic response the equilibrium equation is supplemented by the dynamic blocks, and takes the form:

$$\{P\} = [M] \cdot \{\ddot{u}\} + [C] \cdot \{\dot{u}\} + [K] \cdot \{u\} \tag{1}$$

where {P} is the vector of nodal forces, [M] is the mass matrix, [C] is a damping matrix and {u} is the vector of nodal displacements.

As it has been shown in many studies (for example [25]) for the short–term load the damping effect can be neglected what leads to the simplification of equation (1) to the form:

$$\{P\} = [M] \cdot \{\ddot{u}\} + [K] \cdot \{u\}. \tag{2}$$

After replacing the time derivatives of displacements {ü} by differences displacement {u} in successive discrete moments of time t, the new static equilibrium equation taking into account the inertia forces [M] {ü} is obtained for the each time step and therefore it is possible to apply the algorithms used in the analysis of static. Time integration in the *ANSYS* program is done using the Newmark method and solution of equations in successive time steps is made by Newton–Raphson algorithm. This approach allows analysing the behaviour of the structure subjected to pulse loading.

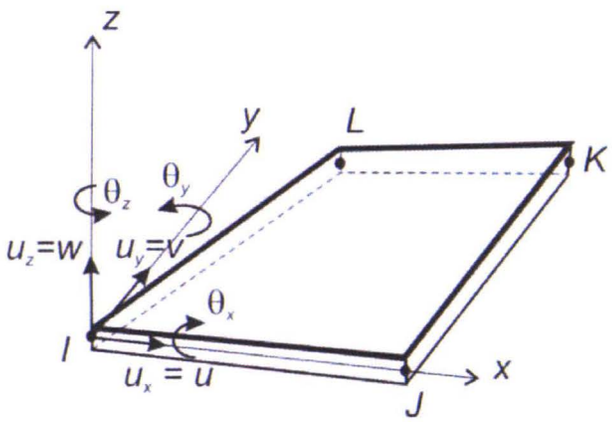

Figure 6 Quadrilateral, four node shell element

Discretization of channel section beam–columns was performed with the quadrilateral; four nodes shell elements (Fig. 6) with six degrees of freedom (three orthogonal displacements and three rotations around the axis in the plane of the element) at each node.

The way of discretization (number and size of elements) was selected on the basis of experience in such a way as to ensure the freedom of the tracking distortion during deformation, that is, during the pulse and after its termination. By default at least 5 elements along one half-wave of sinusoid, occurring during buckling, are assumed. Accepted model for discrete channel section is shown in Fig. 7.

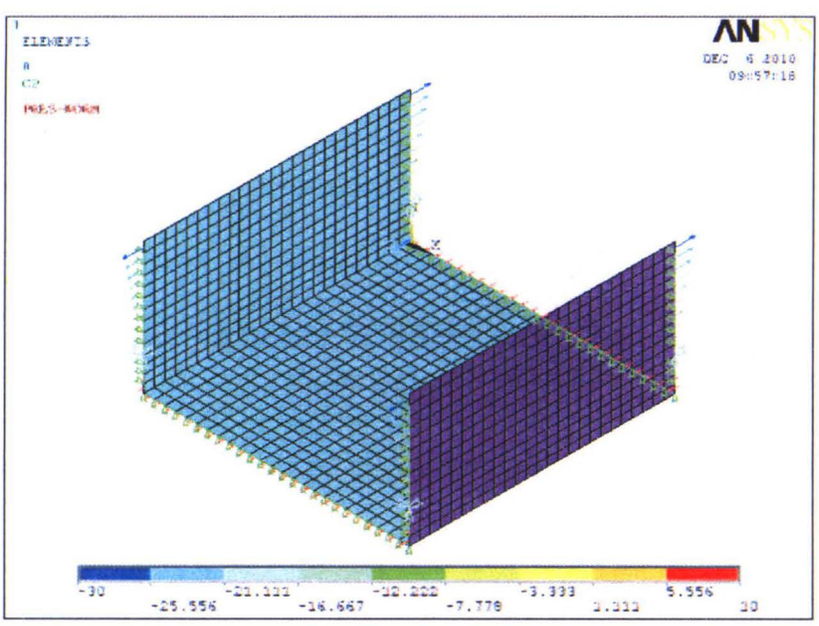

Figure 7 Finite element model of considered channel section girder

For considered girder the boundary conditions corresponding to simple supports are set only at loaded edges.

It was assumed that the bending occurs about an axis, for which the second moment of area is the smallest, and therefore *FEM* model is prepared in this way that on the neutral axis of bending in the ending sections were nodes in which the displacement in the x direction was set to zero (Fig. 8). Rectilinearity of the loaded edges is provided by requiring the permanent displacements of all nodes lying on the edge of the girder in the direction normal to the wall of the girder (Fig. 8). To ensure that deformations are compatible with the deflection in bending the edges normal to the neutral axis remained straight in the plane containing the wall of the column, in addition, for all nodes lying on that edges the constant rotation around the axis parallel to the axis of the neutral section was presupposed.

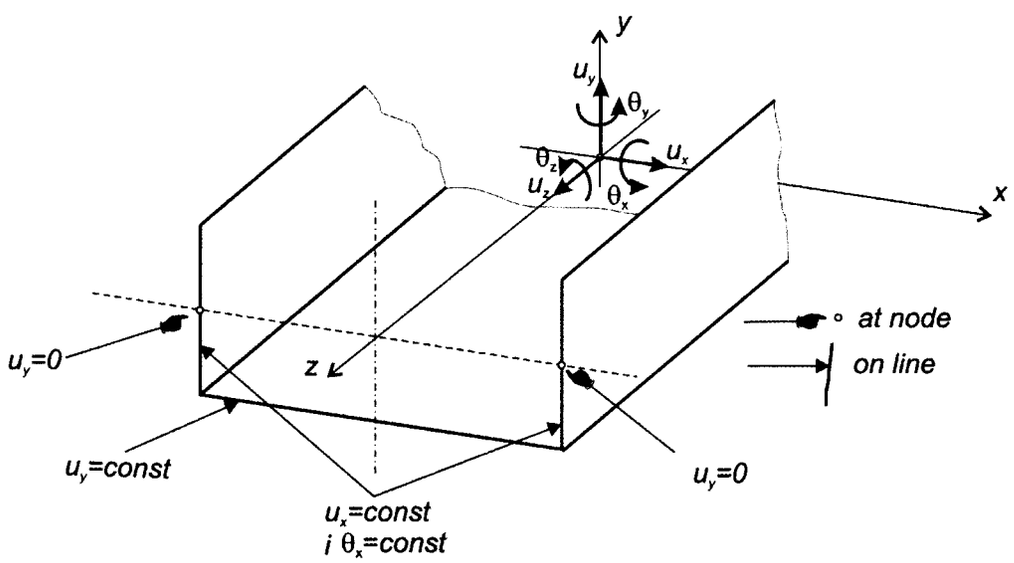

Figure 8 Assumed boundary condition

4. Results of numerical calculation

All presented results were obtained using *ANSYS* software based on finite element method. From linear analysis the critical moment with corresponding buckling mode and modal mode with corresponding natural frequency was obtained. The calculation results are presented in Figs. 9 and 10. The lowest critical moment is equal to $M_{cr} = 27.9$ Nm.

The more similar (maximum deflection on web) modal mode to the lowest buckling mode (Fig. 9) is the third modal mode (Fig. 10c), for which natural frequency is equal $f_3 = 1277$ Hz. Taking the modes similarity into account the period of pulse duration was calculated from period of natural vibration for the third modal mode. For all employed pulses the duration was set to T_p= 0.783 ms. The results presented below were obtained with assumption for amplitude of initial imperfection set to 1/100 wall thickness ($\xi^* = w_{max}/h = 0.01$, where w_{max} – maximum deflection, h – thickness of the girders wall).

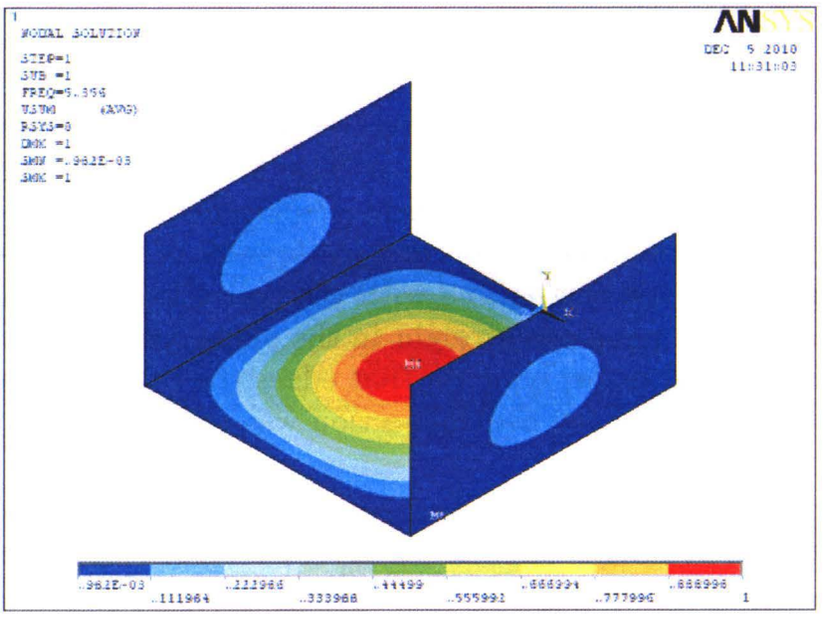

Figure 9 Buckling mode: $M_{cr1} = 27.9$ Nm

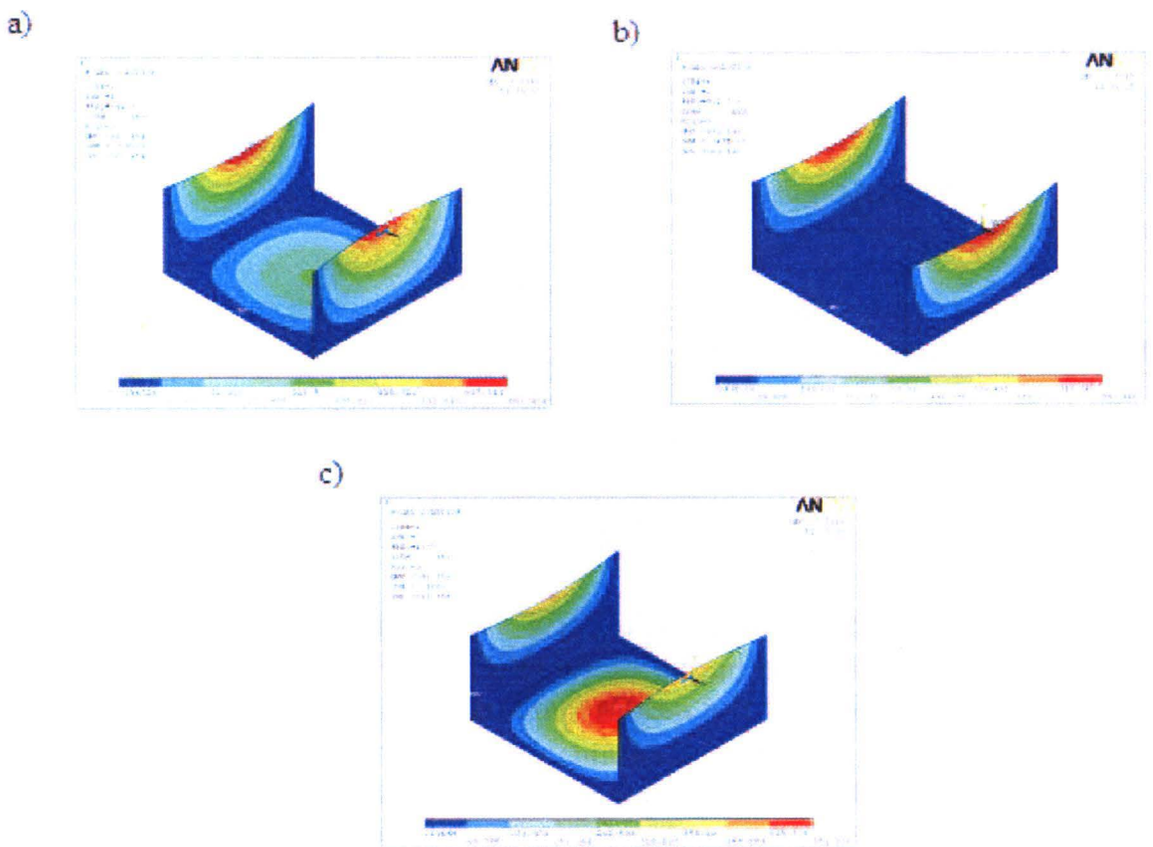

Figure 10 Modal mode: a) $f_1 = 841$ Hz; b) $f_2 = 931$ Hz; c) $f_3 = 1277$ Hz

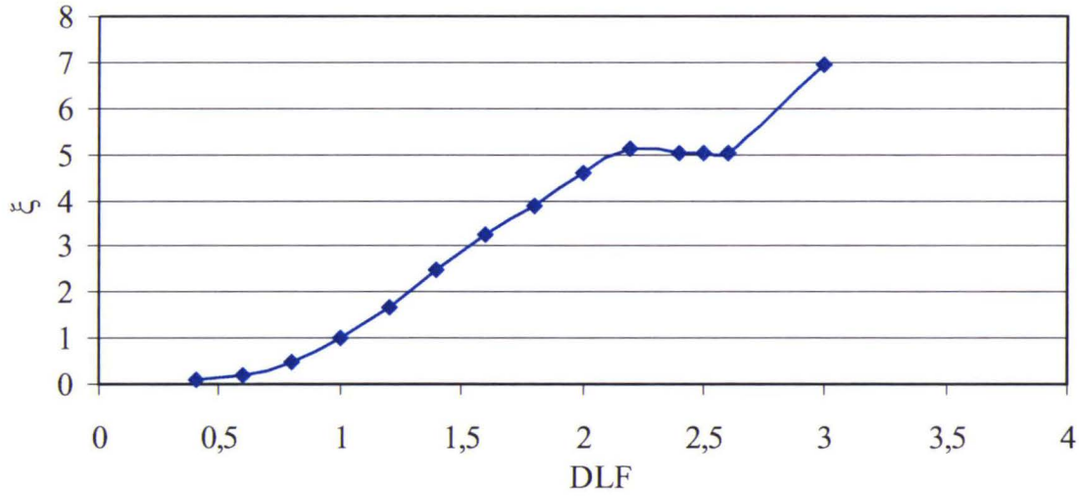

Figure 11 Dimensionless displacement ξ vs. DLF for rectangular pulse loading

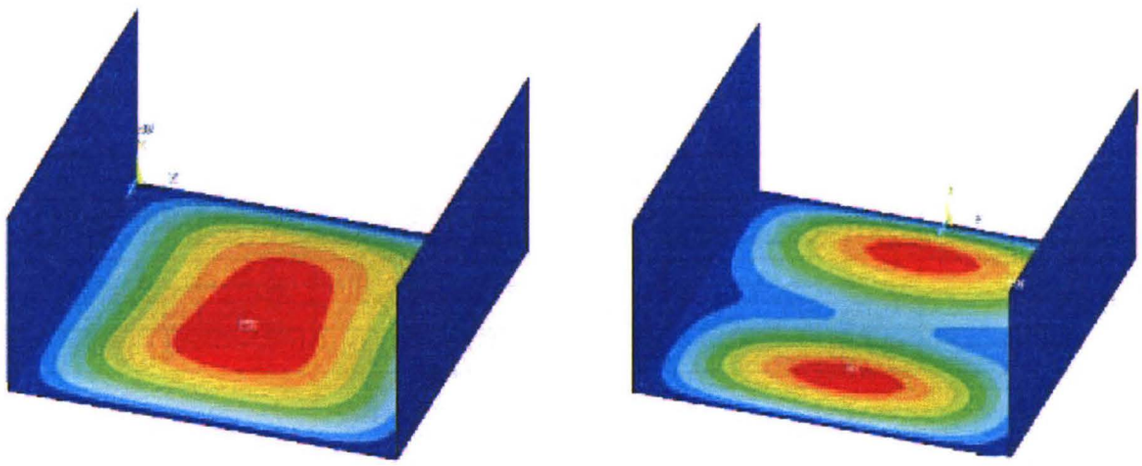

Figure 12 Buckling mode for different dynamic load factor: a) DLF=2.1; b) DLF=2.4

In Fig. 13 the influence of type of the load decrease is presented – the graphs present dynamic responses for three different pulse types: R – rectangular, $0.5T3$ – trapezoidal and $T3$ – triangular (see Fig. 5). All mentioned pulses have the same period of duration and amplitude.

It was difficult to obtain value of critical load for $T3$ pulse based on Budiansky-Hutchinson criterion, because there are two large increases of deflection for DLF=2.7 and DLF=2.9. A critical value DLF_{cr}=2.9 was taken accordingly to Budiansky–Hutchinson criterion which says that the dynamic stability loss occurs when the maximum deflection grows rapidly with the small variation of the load amplitude.

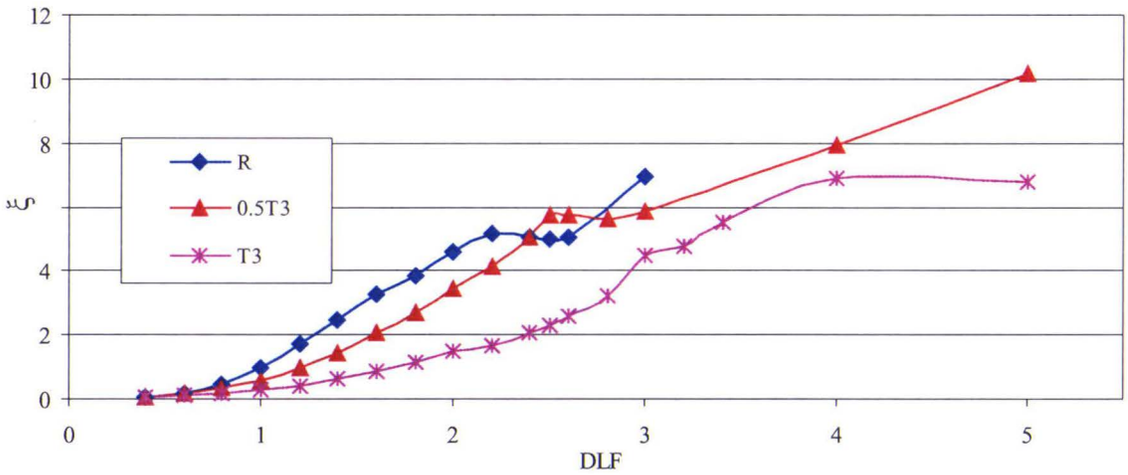

Figure 13 Dimensionless displacement ξ vs. DLF for rectangular R, trapezoidal 0.5T3 and triangular T3 pulse loading

Table 1 Critical value of dynamic load factor for different pulse loading

Pulse type	Dimensionless area under pulse loading curve T_p=const.; N_{x0}=const.	DLF_{cr} for Volmir criterion	DLF_{cr} for Budiansky–Hutchinson criterion	DLF_{cr} for Ari–Gur and Simonetta criterion
R	1	1	1.3	2
0.8T3	0.9	1.1	1.7	2.5
0.5T3	0.75	1.2	1.9	2.6
0.2T3	0.6	1.5	2.7	3
T3	0.5	1.7	2.9	4

In Fig. 14 the influence of load increase in assumed pulses is presented. The relation between dynamic responses is similar to this presented in Fig. 13. It could be said that the critical dynamic load factor as well as dynamic responses (curves in Figs 13 and 14) do not strictly depend on load increase or decrease during the pulse (compare with Fig. 15). The differences in DLF_{cr} appears because all applied pulses have different areas under pulse loading curve – the higher area the smaller DLF_{cr} obtained for considered criterion (Tabs 1 and 2).

In order to present a better comparison of the influence of the shape of pulse loading on critical dynamic load factor, the three triangular pulse shapes (T1, T2 and T3 – Fig. 3) are considered.

All these pulses have the same area under pulse loading curve but different way of the load increase and decrease. The results are presented in Fig. 15 – it can be

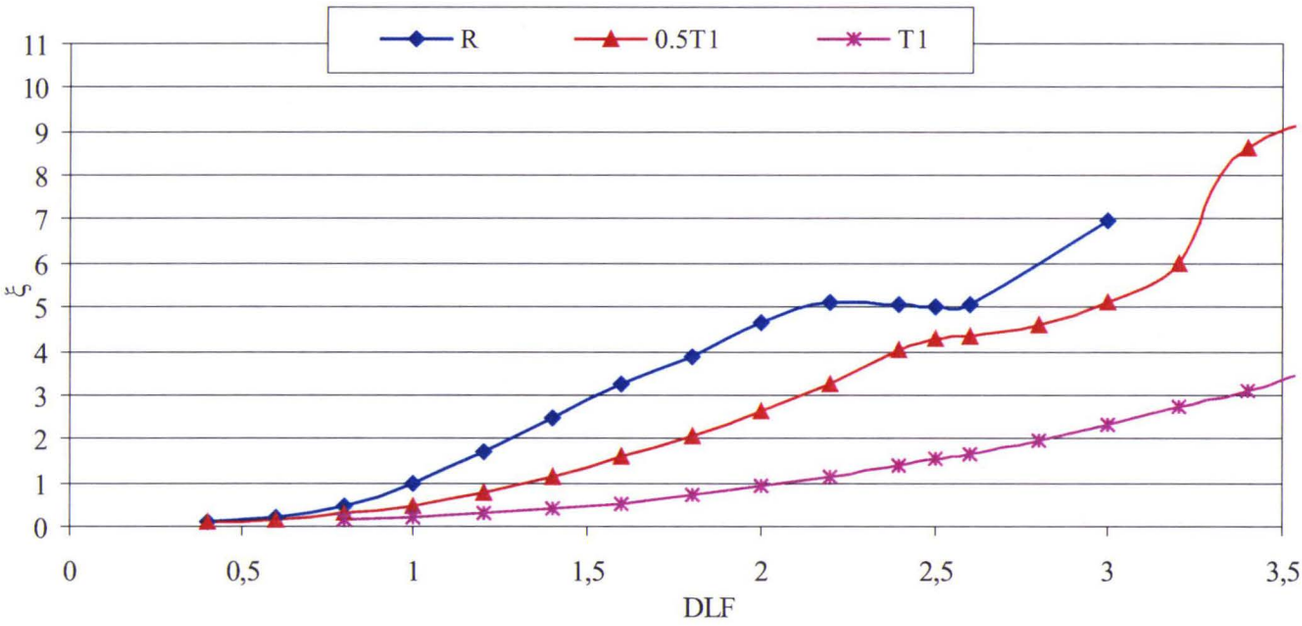

Figure 14 Dimensionless displacement ξ vs. DLF for rectangular, trapezoidal 0.5T1 and triangular T1 pulse loading (see Fig. 4)

Table 2 Critical value of dynamic load factor DLF_{cr} for different pulse loading

Pulse type	Dimensionless area under pulse loading curve T_p=const. N_{x0}=const.	DLF_{cr} for Volmir criterion	DLF_{cr} for Budiansky–Hutchinson criterion
R	1	1	1.3
0.8T1	0.9	1.1	2.1
0.5T1	0.75	1.3	2.3
0.2T1	0.6	1.7	2.7
T1	0.5	2.1	3.1

said that the slope of the load increasing or decreasing have not significant influence on critical dynamic load factor (see Table 3). The influence of pulse duration on dynamic responses has been analyzed. Different pulse duration T_p was analysed (Fig. 16) it can be noted that when duration T_p is extending critical value of dynamic load DLF_{cr} is decreasing. The pulse duration longer than period of natural vibration means that it is almost quasi-static load and curve $\xi(DLF)$ lies closer to static post buckling equilibrium path (see curve denoted by $1.5Tp$ in Fig. 16) and also the DLF_{cr} leads to unity. The case denoted by $1.5T_p$ corresponds to case which pulse duration is equal to period of fundamental natural vibration (f_1 – Fig. 10.)

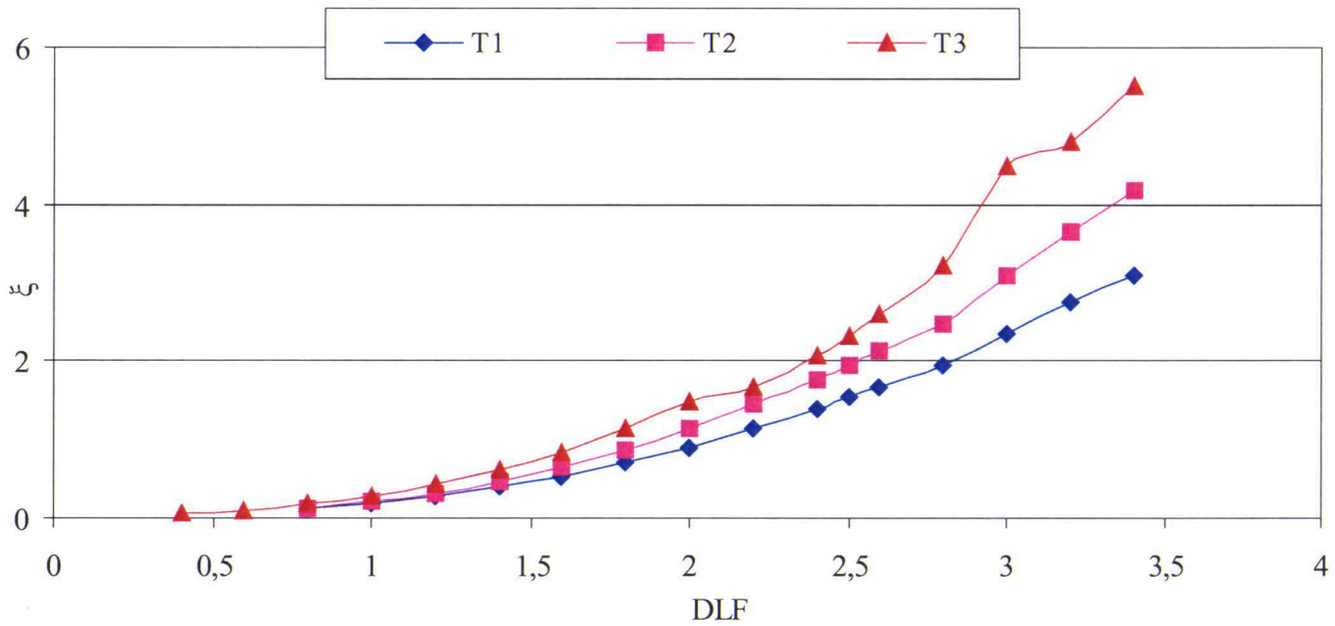

Figure 15 Dimensionless displacement ξ vs. DLF for different triangular pulse loading

Table 3 Critical value of dynamic load factor DLF_{cr} for different triangular pulse loading

Pulse type	Volmir criterion	Budiansky–Hutchinson criterion
T1	2.1	3.1
T2	1.9	2.9
T3	1.7	2.9

Based on Fig. 17 it can be noted that amplitude of initial deflection has a significant influence on value of DLF_{cr}, greater value of initial deflection have effect of lowering critical value of dynamic load factor. The same dependence appears for static load as well as dynamic pulse compression load [22].

There have not been any difficulties in finding the corresponding modal mode and buckling mode in case of compression load, on the contrary when structure is subjected to bending the local buckling mode and the modal mode are different (Figs 9 and 10). That was the reason to investigate the influence of shape of initial imperfection on critical dynamic load factor. The amplitude of initial imperfection have been set to 1/100 wall thickness and the three shapes have been taken into account – shape corresponding to third modal mode (Fig. 10c), first and second buckling mode (Fig. 9). Obtained results are presented in Fig. 18 and Tab. 6. It can be said that the shape of initial imperfection for assumed amplitude have not any influence on dynamic load factor – all curves presented in Fig. 18 lie very close one another.

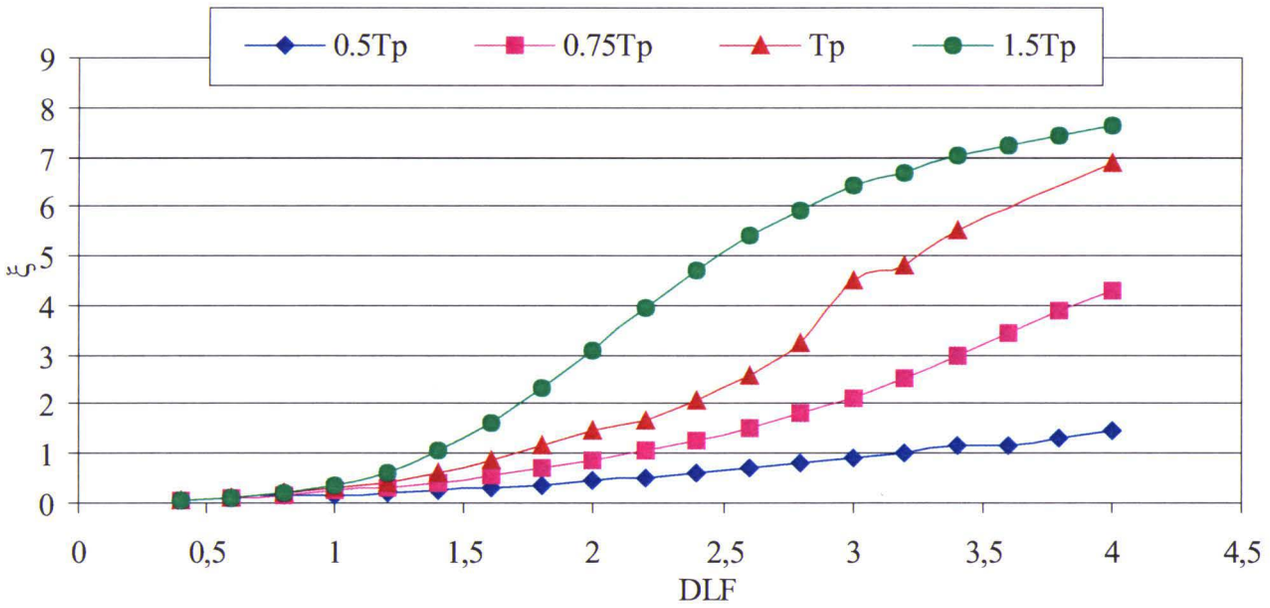

Figure 16 Influence of pulse duration T_p on function ξ vs. DLF for triangular T3 pulse loading

Table 4 Critical value of dynamic load factor DLFcr for different pulse duration

Pulse duration	Volmir criterion	Budiansky-Hutchinson criterion
$0.5T_p$	3.2	3.9
$0.75T_p$	2.2	3.5
T_p	1.7	2.9
$1.5T_p$	1.4	2.1

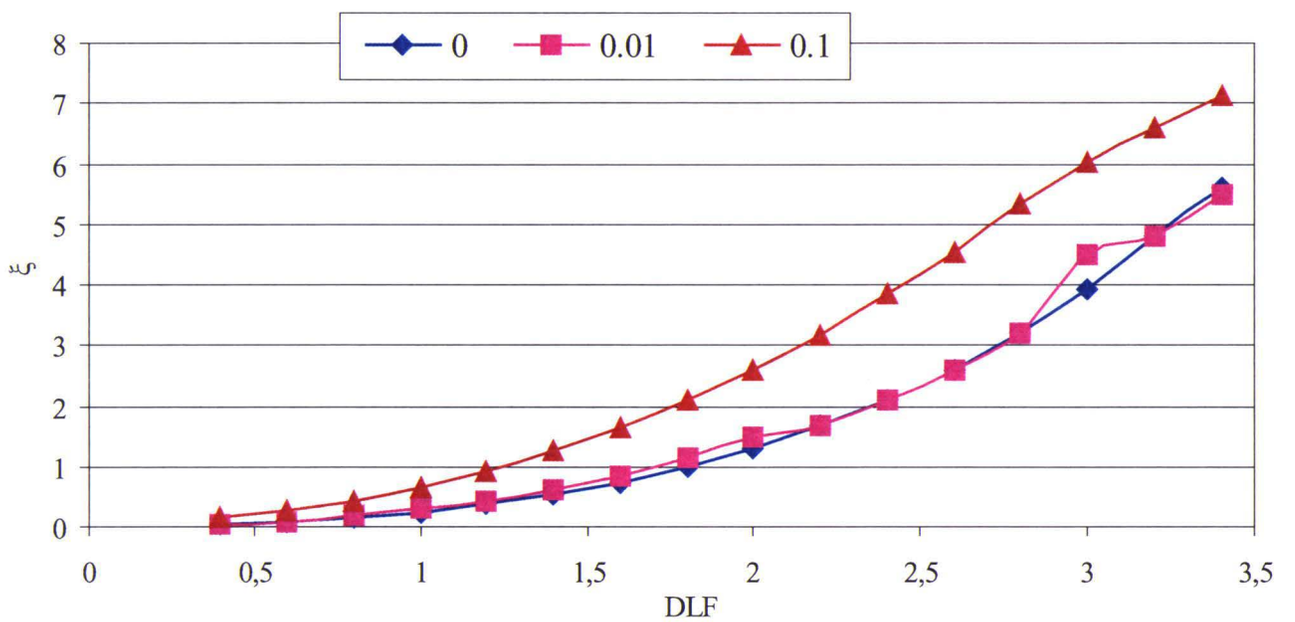

Figure 17 Influence of amplitude of initial imperfection on ξ vs. DLF relation for triangular T3 pulse loading

Table 5 Critical value of DLF for different amplitudes of initial imperfection

Amplitude of initial imperfection	Volmir criterion	Budiansky-Hutchinson criterion
0.1h	1.3	2.5
0.01h	1.7	2.9
0h	1.8	3.1

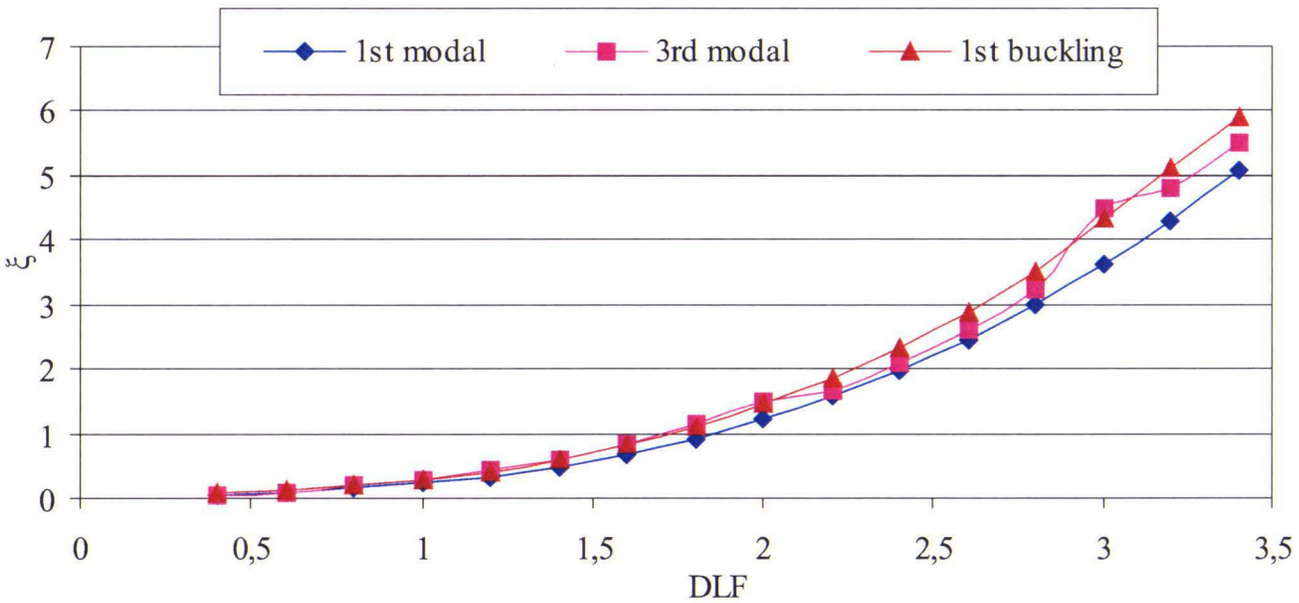

Figure 18 The initial imperfection shape influence on function ξ vs. DLF for triangular T3 pulse loading

Table 6 Critical value of dynamic load factor DLFcr for different shape of initial imperfection

Shape of initial imperfection	Volmir criterion	Budiansky-Hutchinson criterion
1^{st} modal mode	1.8	2.9
3^{rd} modal mode	1.7	2.9
1^{st} buckling mode	1.7	2.9

5. Conclusions

Analyzing the results of calculation for dynamic response for C–shape cross–section girders subjected to bending pulse load and comparing obtained critical dynamic load factors using well–known criteria, it can be stated that:

- the mode of initial imperfection for relatively small amplitude has no significant impact on critical dynamic load factor,
- the value of amplitude of initial imperfection changes the critical dynamic load factor – the higher amplitude the smaller critical dynamic load factor,
- the slope of increasing or decreasing load during pulse loading has very small influence on critical dynamic load factor, the significant effect appears when the area under pulse loading curve is changing – the higher area the smaller DLF_{cr},
- longer pulse duration leads to results similar to one obtained when the structures are subjected to static load – for longer pulse duration the critical dynamic load factor tends to unity.

The above conclusions are similar to results obtained for structures subjected to compressive pulse loading.

References

[1] **Gryboś, R.**: Stateczność konstrukcji pod obciążeniem uderzeniowym, *PWN*, **1980**.

[2] **Jansen, O., Langseth, M. and Hopperstand, O.S.**: Experimental investigations on the behaviour of short to long square aluminium tubes subjected to axial loading, *Int. Journal of Impact Engineering*, 30, pp. 973–1003, **2004**.

[3] **Witmer, E.A. and Pian, T.H.**: Dynamic deformation and buckling of spherical shells under blast and impact loading, NASA TN D-1510, **1962**.

[4] **Timoshenko, S.P. and Gere, J.M.**: Teoria stateczności sprężystej, *ARKADY*, **1963**.

[5] **Volmir, S.A.**: Ustoiczivost deformirujemych system (in russian), *Nauka*, Moskwa, **1967**.

[6] **Volmir, S.A.**: Nieliniejnaja dinamika płastinok i obołoczek (in russian), *Nauka*, Moskwa, **1972**.

[7] **Budiansky, B.**: Dynamic buckling of elastic structures: criteria and estimates, Report SM-7, NASA CR-66072, **1965**.

[8] **Budiansky, B. and Hutchinson, J.W.**: Dynamic buckling of imperfection–sensitive structures, *Proceedings of the Eleventh International Congress of Applied Mechanics*, Goetler H. (Ed.), Munich, pp. 636–651, **1966**.

[9] **Koning, C. and Taub, J.**: Impact buckling of thin bars in the elastic range hinged at both ends, NACA TM 748, **1934**.

[10] **Sevin, E.**: On the elastic bending of columns due to dynamic axial forces including effects of axial inertia, *Journal of Applied Mechanics*, Transactions of ASME, pp. 125–131, **1960**.

[11] **Hutchinson, J. W. and Budiansky, B.**: Dynamic buckling estimates, *AIAA Journal*, 4–3, pp. 525–530, *1966*.

[12] **Huyan, X. and Simitses, G.J.**: Dynamic buckling of imperfect cylindrical shells under axial compression and bending moment, *AIAA Journal*, 35 (8), pp. 1404–1412, **1997**.

[13] **Schokker, A., Sridharan, S. and Kasagi, A.**: Dynamic buckling of composite shells, *Computers & Structures*, 59 (1), pp. 43–55, **1996**.

[14] **Weller, T., Abramovich, H. and Yaffe, R.**: Dynamic buckling of beams and plates subjected to axial impact, *Computers &Structures*, 37, pp. 835–851, **1989**.

[15] **Abramovich H. and Grunwald A.**: Stability of axially impacted composite plates, *Composite Structure*, 32, pp.151–158, **1995**.

[16] **Ari–Gur J. and Simonetta S.R.**: Dynamic pulse buckling of rectangular composite plates, Composites Part B, 28B, pp. 301–308, **1997**.

[17] **Simitses G.J.**: Dynamic stability of suddenly loaded structures, *Springer Verlag*, New York, **1990**.

[18] **Kubiak T.**: Criteria for dynamic buckling estimation of thin–walled structures, *Thin–Walled Structures*, Vol. 45 (10–11), pp. 888-892, **2007**.

[19] **Petry D., and Fahlbusch G.**: Dynamic buckling of thin isotropic plates subjected to in–plane impact, *Thin–Walled Structures*, 38, pp. 267–283, **2000**.

[20] **Kubiak T.**: Dynamic buckling of thin–walled composite plates with varying width-wise material properties, *Int. J. of Solid and Structures*, 45, pp. 5555–5567, **2005**.

[21] **Czechowski L.**: Dynamiczna stateczność w zakresie sprężysto–plastycznym kompozytowych płyt prostokątnych poddanych złożonemu obciążeniu, Łódź, **2007**.

[22] **Kowal–Michalska K.**: Stateczność dynamiczna kompozytowych konstrukcji płytowych, *WNT*, Warszawa, **2007**.

[23] **Kubiak T.**: Dynamic buckling of thin–walled girders with channel cross-section, VDI-Berichte, 1899, pp. 69–78, **2005**.

[24] **Teter A.**: Dynamic, multimode buckling of thin–walled columns subjected to in–plane pulse loading, *Int. J. of Non–Linear Mechanics*, 45, pp. 207 – 218, **2010**.

[25] **Cui S., Hao H., Cheng H.K.**: Theoretical study of dynamic elastic buckling of columns subjected to intermediate velocity impact loads, *Int. J. of Mechanical Science*, 44, pp. 687–702, **2002**.